

Applications of Nuclear Track Detectors in Radiation-Protection Monitoring

Luigi Tommasino

Consultant. Via Cassia 1727, 00123, Roma

(Received 9 December 2011; accepted 16 December 2011)

The present paper deals with the solid state etch-track detectors and their applications to the detection/dosimetry of neutrons, radon, and radon-decay products.

Most of the scientists, actively engaged in the late 60's and in the 70's for monitoring the occupational neutron-exposure by etch-track detectors, became also involved in the development of personal monitors for the exposure to radon-decay products in mines.

The personal dosimetry of neutrons and that of radon decay products have had a parallel history and a lot of common traits, such as the same track detectors, the same etching and counting procedures, the same scientists and/or laboratories involved.

These parallel investigations have been conducive to the development of etch-track-based film-badges for the detection of the neutron fluency and the radon concentration respectively. Thanks to these parallel investigations, it was possible to demonstrate that radon may represent a strong disturbing factor for the response of neutron film-badges. In particular, it was finally possible to explain the erratic response obtained in the past with neutron film-badges, based on polycarbonate track detectors, characterized by a large radon sorption.

Finally, a strategy similar to that established for neutron dosimetry has been recently proposed to solve the long-standing problem of the dosimetry of radon-decay products.

Key words: track detectors, neutrons, cosmic rays, radon

1. Introduction

The response of conventional detectors like gas counters, scintillators, semiconductors, nuclear emulsions, thermoluminescent materials, etc., results from radiation-induced energy deposition in sensitive volumes of macroscopic amount of matter. These detectors are adequate for the dosimetry of sparsely ionizing radiations (X- and γ -rays), which loose energy by fairly random distribution of energy deposition. By contrast, heavily charged particles,

and/or neutron-induced particles interact with matter by depositing high concentrations of ionization energy in microscopic and ultramicroscopic volumes surrounding the tracks, which properties determine the high biological effectiveness of these radiations.

In particular, to provide guidelines for the development of suitable detectors for neutron dosimetry, it is necessary to analyse the differences in the spatial distributions of energy deposition between neutron and γ -interactions with tissue¹⁾. Particular emphasis has been given to these differences in the field of microdosimetry, where an extensive analysis has been made on the local energy depositions both at the cellular and sub-cellular levels²⁾

The comparison between neutron and γ -ray interactions with tissue is illustrated in the diagrams of the upper part of Figure 1^{1, 2)}. These diagrams show two monolayers

Luigi Tommasino: Consultant. Via Cassia 1727, 00123, Roma
E-mail: ltommasino@gmail.com

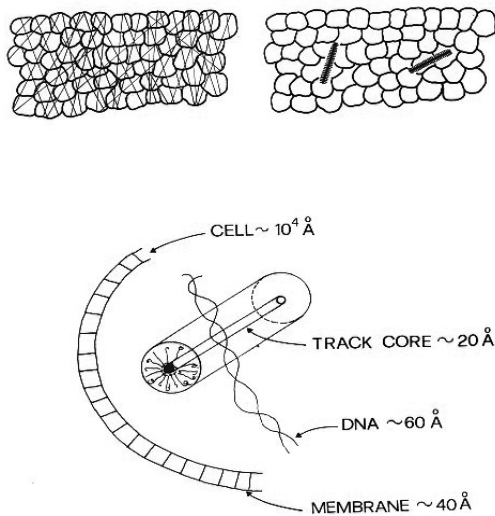


Fig. 1. Upper part: Monolayers of biological cells irradiated respectively to gamma rays (left side) and fast neutrons (right side). Lower side: Single proton track in tissue.

of biological cells (with diameter of about 5 μm) which received a dose of 1 mSv/y of gamma exposure (as typically received from natural terrestrial radiations) and 1 mSv/y of neutrons (as it occurs on high altitudes mountains such as Cervino-Italy³).

The differences appear very clear since, in the case of gamma rays, there is one radiation interaction for every cell in one year, while for neutron irradiation only one out of 2000 cells is crossed by a track which deposits a dose which is about 500 times higher than that due to gammas. The first detector capable of measuring energy depositions in a microscopic element of matter (typically biological tissue) is the Rossi counter^{2, 4}. In fact, this counter has the characteristics that it can simulate a microsphere of biological tissue (namely a cell nucleus).

Advanced portable types of Rossi counters have been developed (known as the tissue equivalent proportional counter-TEPC), which are successfully used for radioprotection dosimetry in mixed field of radiations⁵, such as gamma-neutron fields and/or cosmic rays.

In order to understand the mechanisms of track formation and etchability, it is necessary to refer to the spatial distribution of energy depositions at submicroscopic distances from charge-particle trajectories. The lower part of figure 1 shows a magnified view of a single neutron recoil track (typically 1 MeV proton track in tissue), together with important biological targets like DNA and the cell membrane. This track structure is formed by a track core (characterised by high energy deposition) and delta rays which deliver energy at a distance from the track core. For example, a dose of the order of 1 MGy is deposited at 10 \AA radial distance from 1 MeV proton track in tissue⁶. At such submicroscopic distances from nuclear tracks, the difference between sparse radiation (X- and γ -rays) and high-LET particles are enormous. It is the high energy deposition

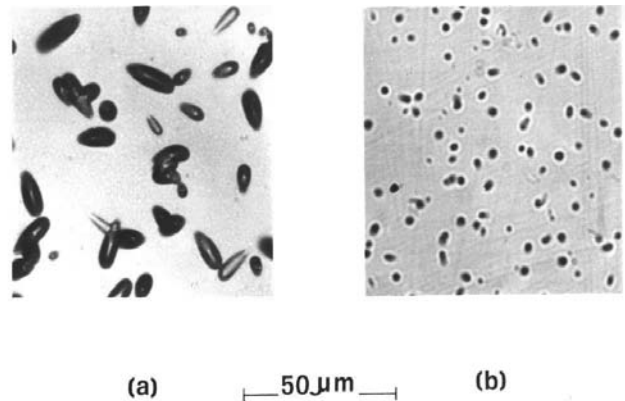


Fig. 2. Fission-fragment tracks (a) and neutron-induced-recoil tracks (b) in polycarbonate.

in the vicinity of the particle trajectory the most crucial quantity for the registration of damage tracks⁷. In fact, the most important characteristic of damage track detectors is that there is a minimum density of damage within an atomic-size volume surrounding the track-trajectory, that will permit the track to be enlarged by etching. The existence of this threshold is one of the most valuable characteristics of damage track detectors, which explains their ability to discriminate against large fluxes of lighter energetic particles, electrons, gamma rays, etc.

By contrast, the responses of detectors with macroscopic volumes are sensitive to the whole energy loss along the track. In situations where the saturation phenomena in the vicinity of the track are predominant, such as with organic scintillators, the response to the outer part of the track is relatively much larger than to the core. For these reasons, the scintillators can be considered to be just the converse of the damage track detectors⁸.

2. Track etching and counting

A track becomes etchable when the rate of etching along the track, V_t , exceeds the rate at which the surface is etched, V_b ⁹. If the track is not perpendicular to the surface, then the component of V_t perpendicular to the surface must exceed V_b for registration to occur. Figure 2 (a) shows tracks of neutron-induced fission fragments entering a polycarbonate detector from a fissile radiator, while Figure 2(b) presents tracks of recoil-particles, induced by neutrons in the detector itself. Since for fission fragments V_t is much larger than V_b the tracks are elongated and well defined. Short etch pits instead of fully developed tracks appear in Figure 2(b), since in this case V_t is not much larger than V_b . For most applications of damage track detectors in dosimetry, it is necessary to evaluate low track densities (1 to 1000 tracks per cm^2) for large number of detector foils). The shortcomings of counting individual track in large detector areas under the microscope have been overcome through the development of the spark counter and of different image analyzer systems for the automatic counting

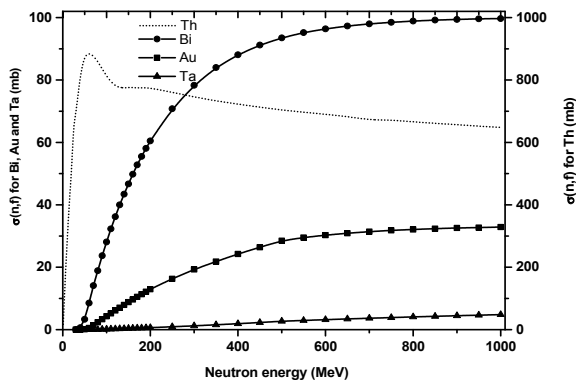


Fig. 3. The neutron fission cross-section, $\sigma(n,f)$, of ^{232}Th , ^{209}Bi , ^{197}Au and ^{181}Ta versus the neutron energy. The right hand ordinate is scaled for the thorium cross-section.

of both chemically and electrochemically etched tracks⁹. These developments have greatly facilitated the applications of track detectors in the measurement of cosmic ray neutrons, in personal neutron dosimetry and in large scale survey of radon in dwellings^{9,10}.

3. Cosmic-ray-neutron measurements by etch-track detectors.

Passive detectors are very attractive for cosmic ray measurements both at aircraft and space altitudes, because of their small size, low weight, lack of need of electrical power and of the stringent requirements for the environmental parameters (temperature, vibration and interference with the on-board instrumentation). Different multidetector stacks have been developed for in-flight measurements, which make it possible to measure low- and high-energy neutrons^{3,10-11}.

These stacks consist of several types of passive detectors for the registration of recoil- and fission-fragment-tracks induced by neutrons. Most of these detectors have been used on earth for the assessment of the occupational exposure⁷, or in outer space for cosmic-ray physics and/or for the assessment of the dose received by astronauts^{9-10,12-13}.

A great deal of efforts and new developments has been required to make these detectors useful for in-flight measurements^{10,14} with special regard to the use of large area stacks. Even though these multidetector systems present the complexity typical of cosmic ray stacks, the scanning of many different types of detectors is relatively simple and rapid, as required for dosimetric applications. In particular, a simple microfiche reader can be useful to scan large areas of different types of neutron detectors for the counting of both fission-induced aluminum spots in spark-counted replicas or electrochemically etched recoil tracks¹⁰.

A major drawback of damage-track detectors is their large and unpredictable background. This problem has been finally solved by using the detection principle of counting coincidence-track events on matched-pair of detectors, not only for long-range particles but also for very short tracks

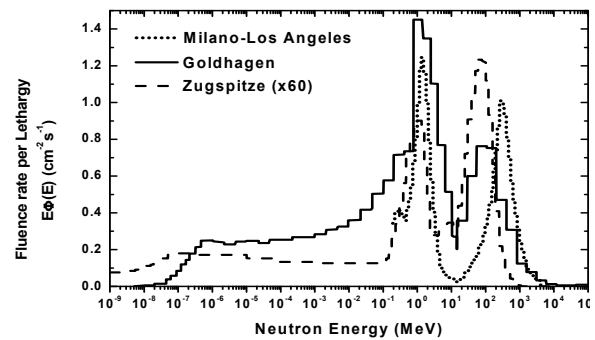


Fig. 4. Three different spectra of cosmic ray neutrons.

such as those induced by neutron recoils¹⁰ which, once etched electrochemically, can be easily seen on the screen of a microfiche reader.

Stack for neutron spectrometry

The basic requirements for a stack for neutron spectrometry (based on the unfolding procedures) is to have different detectors, which have a known response as a function of the neutron energy and chosen in such a way that all the parts of the expected energy range are included. In order to cover both the low- and the high-energy range of neutrons, two categories of detectors have been chosen which are based respectively on the registration of neutron-induced recoil-tracks in organic materials and neutron-induced fission fragments in heavy elements^{10,14}.

Neutron-induced fission cross-sections for some heavy nuclei (^{235}U , ^{238}U , ^{232}Th , ^{209}Bi) are internationally recommended as secondary standards for neutron flux monitoring in the energy region above 20 MeV¹⁰. However, because of the possible concern about the radioactivity of uranium and thorium, they are not useful for onboard measurements. In practice, only bismuth, gold and tantalum films have been used for the detection of high energy neutrons through fission-induced reactions^{10,14}.

These fission-track detectors are very important, since they make it possible to exploit the excellent characteristics of the fission reactions in bismuth, gold and tantalum for the measurements of high energy neutrons, such as:

- excitation functions well above 20 MeV which eliminate the influences of low energy neutrons,
- smooth variation of the cross-section with neutron energy,
- mono-isotopic and non-radioactive materials, which make them easy to transport and handle.

Figure 3 shows the fission-cross section of bismuth, gold, tantalum and thorium respectively¹⁰.

The passive neutron spectrometer based on different types passive track detectors (hereafter referred to as ANPA-stack) is very compact and has a total weight of less than 1 kg¹⁴. The only other neutron spectrometer available consists of multisphere hydrogenous moderators, which are supplemented by different layers of lead shielding to extend the response to high energy neutrons^{15,16}. By contrast with the ANPA-stack, this multisphere spectrometer is so bulky

Table 1. Measured and calculated doses on roundtrips between Europe and Japan at different phases of the solar cycle.

Date	Roundtrip	N° of flights	Measured dose rate H*(10)/t ($\mu\text{Sv h}^{-1}$)	Measured H*(10) (μSv)	(CARI 6) E-(ISO) (μSv)	EPCARD 3.2v (μSv)	
						H*(10)	E
May-July 1997	Milan-Tokyo	8	4.7 \pm 0.4	102 \pm 8	115 \pm 11	122 \pm 11	145 \pm 14
May-July 2001	Paris-Tokyo	10	4.6 \pm 0.6	105 \pm 11			
May 2002	Paris-Fairbanks- Tokyo	1	4.6 \pm 0.8	130 \pm 22	132	122	142
July 2002	Rome-Tokyo	1	4.5 \pm 0.7	101 \pm 16	93	93	109

and heavy that it can't be used in commercial flights. When compared with the multi-sphere spectrometer, the ANPA-stack, in addition to being very light and compact, does not require any technical assistance for on-board measurements. Because of its simplicity and compactness, the ANPA-stack has been exposed on passenger aircrafts simply by asking pilots to take the stack on-board.

Figure 4 shows the neutron spectrum obtained with a passive stack of track detectors flown in the cockpit of an MD-11 aircraft along the route Milan-Los Angeles for a total of 670 hours from November 1993 to May 1994¹⁴.

Two other neutron spectra are reported in Figure 4, both taken by the multisphere spectrometer respectively on the top of the highest mountain (the Zugspitze) in Germany¹⁵ and onboard a dedicated NASA flight¹⁶.

As it appears clear from Figure 4, all the three neutron spectra have a peak at high neutron-energies. This peak is not present in any of the spectra related to low-energy neutron sources, including reactors. Moreover, the spectra obtained by the multisphere spectrometer have different shapes and they are also different from that obtained by the ANPA-stack. In this last spectrum, the peak at high neutron energies is clearly located at about 300 MeV instead of 100 MeV as for the other two spectra. This 300 MeV peak-energy is consistent with the minimum of the neutron cross sections of O, C, and N¹⁹. As an aside, it is also important to mention that the proton fluence at aviation altitudes is peaked around a few hundreds of MeV²⁰.

Stack for cosmic-ray dosimetry

For on-board measurements, the most important quantity for the radiation protection point of view is the cumulative dose per flight²¹. Short-term variation may occur with the instantaneous values of the dose rate specially during the maximum solar activity, which, typically, has little or no effect on the cumulative dose²².

The dosimetric ANPA stack^{23, 24} is by far more simple than that for neutron spectrometry, since it contains only a stack of bismuth-fission detectors. With this bismuth stack, it is possible to measure the cosmic-ray-neutron dose with energy greater than 50 MeV for a single long-haul flight with a standard deviation better than 20%. In practice, this is the only detector, which has its principal response above 50 MeV. For the dosimetry of low-energy

neutrons, this bismuth stack is supplemented by bubble detectors^{23, 24}. Finally, the non-neutron (low-LET) component is measured by TLD detectors²³⁻²⁵.

Within the extensive investigations carried to date, the ANPA-stack has been used on 107 long-haul flights. At geomagnetic latitudes greater than 50°N, the average route doses are not very dependent on the latitude²⁶. For this reason, average dose rates measured on repeated flights along the route Milan-Tokyo give similar results (within 10%) to those measured during the same period along similar high-latitude flights, such as Milan-Los Angeles²⁷.

The cumulative dose and/or the average dose rate at high latitudes are of particular interest for the study of the solar cycle effects on the air crew exposure since, in addition to being little dependent on the latitude, they should be more dependent on the solar activity than the same quantities at low latitudes. The average rates of the route doses (for the return trips Milan-Tokyo, Rome-Tokyo, Paris-Tokyo) measured in terms of ambient dose equivalent-H*(10), by the ANPA-stack are reported in Table 1.

There are a number of computer programs to calculate dose rates and route doses, such as CARI 6 and EPCARD 3.2v respectively²⁸⁻³¹. In Table 1, the effective dose (E) and the ambient dose equivalent-H*(10), evaluated with the above two computer programs are also reported³².

As it appears clear from Table 1, all the measured ambient-dose-equivalent rates are the same within better than 15%. This consistency applies also to the values of the total cumulative dose with the exception of that of the roundtrip Paris-Tokyo via Fairbanks, characterized by a relatively longer roundtrip flight-duration. Good agreement has been also found between measurement results and calculated doses respectively with CARI 6 and EPCARD programs.

From the extensive investigations carried out on the route Rome-Tokyo, all the data (in terms of the ambient dose equivalent) per flight at different phases of the solar cycle, for two different aircrafts (Boeing 747 and 767), and at different locations within the aircraft are the same within less than 20%^{32, 33}.

4. Neutron and radon monitoring: a parallel history

Since their discovery, damage track detectors have been extensively investigated for the solution of the complex

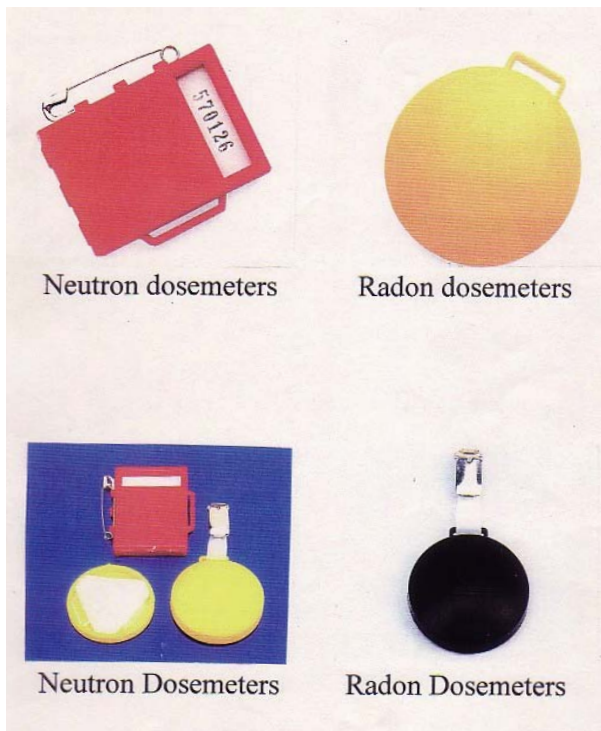


Fig. 5. Different shapes of personal neutron- and radon-dosemeters.

problem of personal neutron dosimetry^{7,9}. In the late 60's and 70's, several laboratories from throughout the world have developed new neutron dosimeters based on damage track detectors^{9,34-38}.

Most of the scientists actively engaged in the late 60's and in the 70's in the solution of the complex problem of personal neutron dosimetry have extended their interests in the field of radon in order to develop individual monitors for the exposure to radon decay products in mines by using the same track detectors^{9,34-38}.

The personal dosimetry of neutrons and that of radon decay products have had a parallel history and a lot of common traits, such as the same track detectors, the same etching and counting procedures, the same scientists and/or laboratories involved. Despite the fact that the dose to neutrons is due to external exposure while that to radon decay products to internal exposure, identical monitoring strategies have been often adopted, within which a given track density is converted into a neutron dose or otherwise into a dose of radon decay products by appropriate conversion coefficients. In the case of radon decay products, this approach has been facilitated by measuring the radon gas concentration (as surrogate), which can be converted into the radon decay product concentration if the equilibrium factor is either monitored or known to have a given value³⁹.

Passive radon monitors are formed by radon diffusion chambers, enclosing a track detector^{40,41}.

These radon monitors have been increasingly successful both for radiation protection monitoring and elsewhere,

because of their simplicity, robustness, and ease of automation of track counting⁴²⁻⁴⁴. For more than one decade, polycarbonate and cellulose nitrate detectors were the most common plastic detectors for both neutron and radon dosimetry. It was only in 1978 that the poly-allyl diglycol carbonate-PADC detector (known with its trade name CR-39: Columbia resin 1939) was first introduced as track detector⁴⁵. Because of the relatively high sensitivity of CR-39 detector it possible to obtain compact passive detector devices. For example, by using CR-39 detectors, a new personal radon dosimeter has been developed at the National Radiological Protection Board-NRPB with such small size of the diffusion chamber that the entire device is compact as any other personal dosimeter for γ , g, and n radiation^{46,47}, as shown in Figure 5. where it can be seen that even the shape and the volume of neutron and radon dosimeters may be identical.

5. Detection of neutrons and radon: The same-type of film badge

In spite of their possible identical geometry, a passive radon monitor is based on a radon diffusion chamber, enclosing a track detector, while a neutron film badge is formed by a solid radiator facing a track detector. However, the first passive radon monitor was termed radon film-badge by Geiger^{48,49}, in analogy with the neutron badge. It consisted of a chamber, into which radon was allowed to diffuse, enclosing a nuclear track emulsion to detect the alpha particles, emitted from radon and its decay products. Because of the shortcomings of the nuclear emulsions, Becker^{50,51} deposited a patent on a similar radon badge, based on etch-track detectors. However, these monitors, instead of radon film badges, should be considered the first in-air radon-diffusion chambers, the principle of which has been exploited in all existing passive radon-monitors^{41,52}.

Finally, truly radon film-badges have been recently proposed, which exploit the radon sorption in solids, which act as radiators in said badges⁵³⁻⁵⁶.

At nanometer scale, these sorption processes can be explained in terms of the radon-atom nanoparticles being enclosed in bulk-distributed nanoholes (absorption) or surface-distributed nanoholes (adsorption). The radon sorption in a given material is expressed in terms of the radon partition coefficient, which is given by the ratio of the radon concentration in the given material to that of the surrounding air. Under equilibrium-absorption conditions, the partition coefficient of plastic materials is referred to as radon solubility, as in liquids⁵³. Incidentally, all types of plastics in their rubbery states can be considered liquid-like materials.

Among the plastics used for track registration, polycarbonate present the largest values of the radon partition coefficient, while CR-39 the lowest⁵³. Measurements of the radon partition-coefficient have been carried out for different types of polycarbonate films from Bayer AG (Makrofol DE, Makrofol G, Makrofol KG, Makrofol N), the values of which

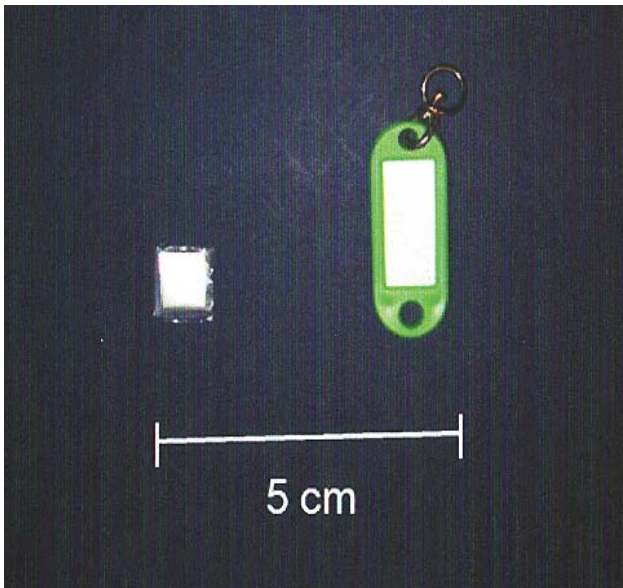


Fig. 6. A compact Rn-monitor (left-hand side) and the same monitor enclosed in a key ring (right-hand side).

have resulted in the range from about 30 to about 90⁵³⁻⁵⁶).

According to the above results, the CR-39 is the most suitable as a detector of the radon film-badge, while the polycarbonate is the most valuable as radiator⁵⁶.

The track detector response can be considered proportional to the radon partition coefficient or to the radon solubility of the radiator⁵³⁻⁵⁶.

Because of the availability of materials with a wide range of partition coefficients (with values from 1 to 2000), it is possible to obtain passive radon monitors with any desired response sensitivity, which is highly valuable, because of the large variability of the radon concentrations, which can be encountered in nature⁵³⁻⁵⁶.

The newly developed badges make it finally possible to overcome all the shortcomings of existing passive radon monitors. In particular, with these monitors it is possible to measure short- and long-term exposures of radon outdoors, indoors, in soil, and in water. For in-water radon measurements, the radon film-badge is just enclosed in a heat-sealed polyethylene bag⁵³.

The left-hand side of Figure 6 shows a uniquely compact radon film badge enclosed in a small plastic bag, while the right-hand side shows a key-ring label containing the same radon film badge. This label-enclosed radon badge shows promise for application as back-up detector, highly valuable for all those measurements, which can't be carried out with existing diffusion-chamber-based monitors. Once proved successfully as back-up detector, this radon film-badge should not take a long time prior to become the principal and/or universal radon monitor.

6. Neutron response of radon film-badges and radon response of neutron film-badges

Very often in this paper, it was emphasized that there are several common traits between the personal dosimetry of neutrons and radon, obtained etch-track detectors.

The use of damage track detectors both for neutron- and radon-dosimetry obviously implies that passive radon dosimeters are also sensitive to neutrons.

Special care should be taken when passive radon dosimeters are used in places where neutron radiations are likely to be encountered, such as in the nuclear industry, in the surroundings of high energy X-ray facility where neutrons are produced by (γ, n) reactions, and around high-energy-particle accelerators.

Moreover, neutrons represent also an important component of the cosmic rays, the intensity of which increases with altitude and latitude. To study the cosmic-ray-neutron response of passive radon monitors⁵⁷, sets NRPB/SSI radon monitors have been exposed at an experimental facility at CERN, which simulates the cosmic-ray-neutron field⁵⁸.

The response, ϵ , per unit of neutron dose of these radon monitors is:

$$\epsilon_{\text{Rn}} = (135 \pm 16) \text{ Tracks}/(\text{cm}^2 \text{ mSv})$$

On the basis of this neutron response and considering a world-wide average of 80 μSv cosmic-ray neutrons at sea level⁵⁹, it is possible to evaluate that, on the average, only about (11 ± 2) tracks/ cm^2 per year can be induced in CR-39. According to the cosmic-ray-background data from UNSCEAR 2000⁵⁹, this CR-39 track-density per year increases to about (31 ± 4) at Mexico-city altitude (2,240m.) and to about (82 ± 10) at La Paz altitude (3400m.). In a long-haul flight from Milan to Tokyo or from Milan to Los Angeles^{10, 32}, the track-density induced by cosmic-rays neutrons in CR-39 is about (3 ± 1) tracks/ cm^2 .

In practice, by using the NRPB/SSI radon monitor for a long-term (six-months) exposure at high altitude (La Paz), the cosmic-ray-neutron-induced tracks is equivalent to a radon concentration of about (3 ± 1) Bq/ m^3 . In brief, it is safe to conclude that the cosmic-ray-neutrons have a negligible effect on the passive radon monitor response even at high altitudes.

By contrast with the cosmic-ray neutron-background, the radon concentrations are unpredictable and may vary from tens of Bq/ m^3 up to several thousands of Bq/ m^3 . Special care is thus required to protect the neutron film-badges from radon exposures.

Recent investigations on the radon partition coefficient of the boron-loaded polystyrene films, used as radiators for neutron badges^{60, 61}, have proved that these neutron badges can be also considered as sensitive radon badges⁵⁶.

Moreover, radon absorption in the detector itself may represent a strong disturbing factor for the response of neutron detectors.

As mentioned earlier, CR-39 and Polycarbonate detectors are characterized by the lowest and the largest radon partition coefficients among plastics^{53, 62, 63}.

Because of the large radon absorption in polycarbonate, it is possible to explain the erratic response of polycarbonate-based neutron badges⁶⁴ in some long-term-integrated

neutron exposures.

Hofert⁶⁴ carried neutron measurements at CERN facilities by three different neutron film-badges, based respectively on CR-39, polycarbonate and nuclear emulsions.

The data with polycarbonate neutron film-badges were not consistent with those obtained with the other two passive neutron badges. However, since then it was suspected that the erratic results, obtained with polycarbonate, might have been due to radon exposures.

The strong effects of the radon exposure on the polycarbonate neutron dosimeter can be drastically reduced, by using an etchant made of a water-based KOH solution⁶⁵. With this etchant, it is possible to register only tracks of neutron-induced recoils of carbon- and oxygen-nuclei. Alpha-tracks in polycarbonate can only be registered when alcohol is added to the KOH solution, as in the case of the polycarbonate neutron dosimeter used at CERN⁶⁴⁻⁶⁶.

A typical neutron film-badge is based on a CR-39 detector facing a polyethylene radiator⁶⁷⁻⁶⁸. The response of this neutron badge is:

$$\epsilon_n = (0.04 \pm 0.01) \text{ Tracks m}^3 / (\text{cm}^2 \text{ kBq h})$$

According to the world-wide indoor radon-concentration of 39 Bq/m³⁵⁹, the tracks, produced in the above neutron film badge, can be estimated to be (14 ± 3) tracks/cm² per year. While this track density can be considered negligible, the real problem arises because the radon concentrations are unpredictable and very high concentrations may be easily encountered. In order to overcome the strong radon-disturbing factor on the neutron-badge response, it is necessary to enclose these neutron film badges in radon free containers^{52-56, 64, 66}.

7. Dosimetry of neutron and radon decay products: a similar strategy

A neutron-detection badge makes it possible to detect only the neutron fluency. Since the dose equivalent is strongly dependent on neutron energy, the evaluation of the dose on the basis of the neutron fluency requires a detailed information on workplace fields (field spectrometry) to evaluate the neutron quality factor and/or the appropriate dose conversion coefficient. In order to avoid the complex task of carrying out the neutron spectrometry, efforts have been made to obtain detector response (number of detected tracks per unit area) which closely matches the strong dependence of the dose conversion coefficient versus the neutron energy^{67, 68}. This is done by choosing suitable reactions, radiator materials, detectors, processing and counting methods. Most of the development work in neutron dosimetry is based on this principle^{9, 67, 68}.

A strategy similar to that established for neutron dosimetry has been recently proposed by Mishra et al.⁶⁹ to solve the long-standing problem of the dosimetry of radon-decay-products. In this case, the dose equivalent of radon-decay products depends strongly on the sizes of airborne particles.

Airborne particles may have sizes from about 1 nm

to tens of microns. These particles can be classified in two broad categories according to their deposition mechanisms, by using the size of 0.25 micron as a benchmark^{69, 70}. This benchmark is justified by the fact, that particles with sizes less than about 0.25 microns are characterized mainly by diffusion-based deposition-mechanisms, and can be termed nanoparticles. The remaining particles (with sizes > about 0.25 microns) are characterized by gravitational-dominated deposition mechanisms and may be referred to as microparticles (i.e. particles with micrometer sizes). This type of characterization is of interest, since the deposition of airborne particles is an important parameter for the assessment of their effects on any target site (skin, lung, technological surface, museum artifact/painting, etc.). Mishra et al.⁶⁹, by using a screen capped bare radon film-badge, have proved that it is possible to simulate the lung deposition of airborne nanoparticles. This screen capped track detector makes it finally possible to obtain a passive monitor of radon decay products, the response of which closely mimics the strong dependence of the dose conversion factor versus the particle sizes.

References

1. Tommasino L (1981) Needs and possibilities for personnel dosimetry and area monitoring of fast neutrons. In the proceedings of the "Fourth Symposium on Neutron Dosimetry. Munich, Neuheberg 1-5 June, pp. 591-503
2. Rossi H-H (1979) The role of microdosimetry in radiobiology. *Radiat. Environ. Biophys.* 17: 29-40
3. Tommasino L, et al (1996) Passive multidetector stack for the assessment of aircrew exposure. *Env. Internat.* 22: pp.S115-S119
4. Rossi H-H (1959) Specification of radiation quality. *Radiat. Research* 10, pp 522-535
5. Schmitz Th, et al (1995) Design, construction and use of tissue equivalent proportional counters. *Radiation Protection Dosimetry*, 61(4): 121-131
6. Tommasino L (1987) Recent trends in radioprotection dosimetry: promising solutions for personal neutron dosimetry. *Nuclear Instruments and Methods in Physics Research A255*: pp293-297
7. Fleischer R-L, Price P-B and Walker R-M (1975) *Nuclear Tracks in Solids: Principles and Applications*. (Berkeley: University of California Press)
8. Price P-B (1981) Applications of plastic track detectors to atomic, nuclear particle and cosmic ray physics. In *Proc. 11th Int. Conf. of Solid State Detectors*, Bristol, (Oxford: Pergamon) pp. 737-755
9. Griffith R-V and Tommasino L (1991) Etch track detectors in radiation dosimetry. In *The Dosimetry of Ionising Radiations vol. III*, pp.323-426, Editors K. Kase, B.B: Bjargard and F.H. Attix. Academic Press, Berkeley
10. L Tommasino L (2004) Detectors/dosimeters of galactic and solar cosmic rays. *Radiation Protection Dosimetry*, Vol. 109, N° 4: pp.365-374
11. Byrne J, et al (1995) New Method for the Rapid Evaluation of Z>1 Cosmic Ray Particles- Results from a Balloon Borne Experiment. *Radiat. Meas.* 25: pp 471-474.
12. Frank A-L, et al (1996) Neutron fluencies and dose equivalents measured with passive detectors on LDEF. *Radiation*

- Measurements 26: pp.833-839.
13. O'Sullivan D and Zhou D (1999) Overview and present status of the European Commission research programme. *Radiat. Prot. Dosim.* 86: pp.279-283.
 14. Tommasino L, et al. (2003) Cosmic ray spectrometry by solid state detectors. *Radiation Measurements* 36: pp.307-311
 15. Schraube H, et al. (1997) The cosmic ray induced neutron spectrum at the summit of the Zugspitze (2963 m). *Radiat. Prot. Dosim.*, 70: pp.405-408.
 16. Goldhagen P (2000) Overview of aircraft radiation exposure and recent ER-2 measurements. *Health Phys.*, 79: pp.526-544.
 17. Tommasino L (1999) In-flight measurements of radiation fields and doses. *Radiat. Prot. Dosim.*, 86: pp.297-301.
 18. A. Zanini A, et al. (2001) Neutron spectrometry at various altitudes in atmosphere by passive detector technique. *Il Nuovo Cimento* 24: pp.691-697
 19. Savitskaya E-N and Sannikov A-V (1995) High energy neutron and proton kerma factors for different elements. *Radiat. Prot. Dosim.* 60: pp.135-146
 20. Heinrich W, Roesler S. and Schraube H (1999) Physics of cosmic radiation fields. *Radiat. Prot. Dos.* 86: pp.253-258.
 21. Bartlett D-T (1999) Radiation protection concepts and quantities for the occupational exposure to cosmic radiation. *Radiat. Prot. Dosim.* 86: pp.263-268.
 22. Lantos P and Fuller N (2003) History of the Solar Particle Event Radiation Doses on-board Aeroplanes using a Semi-empirical Model and Concorde Measurements. *Radiat. Prot. Dos.* 104: pp.199-210.
 23. Curzio G, et al. (2001) The Italian national survey of aircrew exposure: i characterization of advanced instrumentation. *Radiation Protection Dosimetry.* 93: pp.115-123.
 24. Curzio G, et al. (2001) The Italian national survey of aircrew exposure: ii on-board measurements and results. *Radiation Protection and Dosimetry.* 93: pp.125-133.
 25. Lucas A-C (1991) Hypersensitive dosimeters. *Radiat. Prot. Dos.* 35: pp.219-223
 26. Schrewe U-J (1999) Radiation exposure monitoring in civil aircrafts. *Nucl. Instr. and Meth. In Physics Research A* 422: pp.621-625.
 27. L (1999) In-flight measurements of radiation fields and doses. *Radiat. Prot. Dos.*, 86:297-301.
 28. O'Brien K, et al. (1996) Atmospheric cosmic rays and solar energetic particles at aircraft altitudes, *Environment International* 22, Suppl 1: pp.539-544.
 29. Schraube H et al. (2000) Aviation route dose calculation and its numerical basis, in Proceedings of the 10th International Congress of the International Radiation Protection Association, Hiroshima, Japan. T-4-4, P-1a-45, p 1-9 (<http://www.oita-nhs.ac.jp/%7Eirpa10/CD-ROM/Full/t4.html>).
 30. Ferrari A, Pelliccioni M and Rancati T (2001). Calculation of the radiation environment caused by galactic cosmic rays for determining air crew exposure. *Radiat. Prot. Dosim.* 93: pp.101-114.
 31. Roesler S, Heinrich W and Schraube H (2002) Monte Carlo calculation of the radiation field at aircraft altitudes. *Radiat. Prot. Dosim.* 98: pp.367-388.
 32. Tommasino L, et al. The assessment of aircrew exposure throughout a complete solar cycle. Paper presented at the 11th International Congress of the International Radiation Protection Association (IRPA11), Madrid, Spain, 23-28 May (2004)
 33. Tommasino L, et al (2004) Passive multidetector system-ANPA-stack. In the final report of the WG 5. *Radiation Protection* 140: pp.169-179.
 34. Becker K (1969) Alpha particle registration in plastics and its applications for radon and neutron personal dosimetry. *Health Physics* 16: pp.113-123.
 35. Somogy G (1977) Processing of plastic track detectors. *Nucl. Track Detect.* 1: pp.3-20
 36. Cross W-G and Tommasino L (1970) A rapid reading technique for nuclear particle damage tracks in thin foils. *Radiat. Effects* 45: pp.85-89
 37. Tommasino L (1970) Method and apparatus for electrochemical development of damage tracks produced by radiation on insulating materials. Italian Patent N° 51929/70
 38. Sohrabi M (1974) The amplification of recoil particle tracks in polymers and its application in fast neutron personnel dosimetry. *Health Phys.* 27: pp.598-605.
 39. Dixon D-W (1999) A stratified approach to individual dosimetry for radon daughters in mines. *Radiat. Prot. Dosim.* 82: pp.192-200
 40. Fleischer R-L, et al. (1980) Dosimetry of environmental radon: Methods and theory for low-dose integrated measurements. *Health Physics* 39: pp.957-967
 41. R-L Fleischer (1988) Radon in the environment – opportunities and hazards. *Nucl. Tracks Radiat. Meas.* 14: pp.421-435
 42. Fleischer R-L, Hart H. R-Jr and Mogro-Campero A (1980) Radon emanation over an ore body: Search for long-distance transport of radon. *Nucl. Instr. Meth.* 173: pp.169-181
 43. Furlan G and Tommasino L Eds. (1991) Proc. 2nd Workshop on radon monitoring in radioprotection, environmental and/or earth sciences. Trieste, World Scientific, Singapore.
 44. Durrani S-A and Ilic R (1997) Radon measurements by etched track detectors: applications in radiation protection, earth science, and the environment. World Scientific, Singapore
 45. Carwright B-G, Shirk E-K and Price P-B. (1978) A nuclear-track-recording polymer of unique sensitivity and resolution. *Nucl. Instrum. Methods.* 153: pp.457-462
 46. Frank A-L and Benton E-V (1977) Radon dosimetry using nuclear track detectors. *Nucl. Track Detect.* 1: pp.149-179
 47. Bartlett D-T, et al. (1986) A radon personal dosimeter for miners. *Nucl. Tracks* 12: pp.721-724
 48. Geiger E-L (1966) Radon dosimeter. US Patent N° 3,283,153
 49. Geiger E-L (1967). Radon film badge. *Health. Physics.* 13: pp.407-411
 50. Becker K-H (1968) Personnel radon dosimeter. US Patent N° 3,505,523
 51. Becker K-H (1969) Alpha-particle registration in plastics and its applications for radon and neutron personal dosimetry. *Health Physics* 16: pp.113-123
 52. Tommasino L (2001) Personal dosimetry and area monitoring for neutrons and radon in workplaces. *Radiat. Meas.*, 34: pp.449-456
 53. Tommasino L, Tommasino M-C and Viola P (2009) Radon film-badges by solid radiators versus existing passive radon monitors. *Radiat. Meas.* 44: pp.719-723.
 54. Tommasino L, Tommasino M-C and Espinosa G (2010) Radon film-badges based on radon-sorption in solids: A new field for solving long-lasting problems. *Rivista Mexicana de Fisica* S56 (1) 1-4, Febrero
 55. Tommasino L (2010) Radon film-badges versus existing passive monitors based on track-etch detectors. *Nukleonika*, 55: pp.549-553.
 56. Tommasino L, Tokonami S (2011) Four passive sampling elements (quatrefoil) II. Film badges for monitoring radon and

- its progeny. Rad. Prot. Dos. 145: pp.284-287.
57. Orlando C, et al. (2002) A passive radon dosimeter suitable for workplaces. Rad. Prot. Dos. 102: pp.163-168
 58. Mitaroff A and Silari M (2000) The CERN-EU high-energy reference field (CERF) facility for dosimetry at commercial flights altitudes and space. Rad.Prot. Dos. 102: pp.7-22.
 59. United Nations Scientific Committee on the Effects of Atomic Radiation (2000)-UNSCEAR Report 2000 to the General Assembly . Annex B. Exposure to natural radiation sources.
 60. Zapparoli G, et al. (1986) Additional results with electrochemically etched CR-39 neutron dosimeters. Nuclear Tracks.12: pp.675-678.
 61. Mameli A, et al. (2008) CR-39-detector-based thermal neutron flux measurements in the photo neutron project. Nuclear Instruments and Methods in Physics Research. 266: pp.3656-3660.
 62. Moore H and Hubbard L M (1997) ²²²Rn absorption in plastics holders for alpha track detectors: A source of error. Rad. Prot. Dosim. 74: pp.85-91.
 63. Pressianov D, et al. (2000) Polycarbonate: a long-term highly sensitive radon monitor. Nucl. Instrum. Meas. A 447: 619-621.
 64. Hofert, M. (1991) A long-term study of personal neutron monitors in stray fields around high-energy proton accelerators. Radiat. Prot. Dosimetry, 37: pp 261-266
 65. Tommasino L (2004) Electrochemical etching processes for the detection of neutrons and radon-decay products. Nuclear Technology and Radiation Protection 1: pp.12-19
 66. Piesch E, Al-Najjar S-R and Josefowicz K (1991) The two-step electrochemical etching technique applied for polycarbonate etched-track detectors. Nucl. Tracks Radiat. Meas. 19: pp 205-210.
 67. Tommasino L and Harrison K-G (1985) Damage track detectors for neutron dosimetry. I registration and counting methods. Rad. Prot. Dos., 10: pp-207-218
 68. Harrison K-G and Tommasino L (1985) Damage track detectors for neutron dosimetry. II Characteristics of different detection systems. Rad. Prot. Dosim.,10: pp 219-235.
 69. Mishra R, Mayya Y-S and Tommasino L (2011) Mimicking lung dose by wire-mesh capped deposition sensors: a new dosimetric strategy of radon (thoron) decay products. Accepted for publication in the journal Radiat. Prot. Dosimetry
 70. Tommasino L and Tommasino M C (2009) Four sampling-elements, termed quatrefoil, for the collection of radon, its decay products, and other airborne radionuclides. International Patent Application n° PCT/IT/2009/000568.